Reactive Processing of Environmentally Conscious, Biomorphic Ceramics from Natural Wood Precursors

M. Singh and Bo-Moon Yee*
QSS Group, Inc.
NASA Glenn Research Center
Cleveland, OH 44135 (USA)

Abstract

Environmentally conscious, biomorphic ceramics (Ecoceramics) are a new class of materials that are manufactured from renewable resources and wastes. In this study, silicon carbide and oxide-based biomorphic ceramics have been fabricated from pine and jelutong wood precursors. A carbonaceous preform is produced through wood pyrolysis and subsequent infiltration with oxides (ZrO_2 sols) and liquid silicon to form ceramics. These biomorphic ceramics show a wide variety of microstructures, densities, and hardness behavior that are determined by the type of wood and infiltrants selected.

Introduction

In recent years, there has been an increasing interest in using biomimetic-based processing approaches to fabricate a variety of oxide and non-oxide based structural and functional materials. Environmentally conscious ceramics (Ecoceramics) are a class of materials that can be manufactured from renewable resources such as wood. Through pyrolysis of wood, a carbonaceous preform is produced. It is then infiltrated with oxides and non-oxides that react to form a strong and tough ceramic or composite that can be used for a variety of applications including filters and catalyst support, automotive components, tooling and wear components, armor, and lightweight, porous ceramics for aerospace systems [1-12]. Ecoceramics have several benefits over traditional ceramics.

* Summer Intern, Currently at University of Illinois at Urbana-Champaign, IL

The entire manufacturing process can be performed under 1450°C, so the total amount of energy consumed is low. Another benefit is the wide variety of microstructures that can be obtained, determined by the type of wood selected. The use of wood provides a low-cost starting material that has near-net and complex shape capabilities, instead of the simple shapes that are normally produced by traditional ceramic processing techniques.

With the many benefits of using wood as a material, it is critical to have a greater understanding of its structure. Wood is classified as a composite material that behaves anisotropically with a cell morphology that varies with each species [5]. It is composed of cellulose, hemicellulose, and lignin, which decompose to produce char in the form of amorphous carbon during pyrolysis and produces an anisotropic cellular structure. Further information on pyrolysis can be found in the literature [13]. Anisotropy in wood is the result of the orientation and alignment of cells and cell walls, as well as variation in density [14].

Trees are separated into two classes: hardwoods and softwoods. The terms hardwood and softwood do not refer to the hardness of the wood, but relates to the anatomical structure of the tree. Both classes of woods have tubular cells that run in the direction of tree growth, but hardwoods have large porous structures that provide channels for water or sap, while softwoods do not. The channels that run parallel to the growth direction are referred to as longitudinal cells, while ray cells run radially outwards from the center of the tree. Longitudinal cells outnumber the ray cells to varying degrees among species, but the ray cells contribute to the strength in the radial direction [14].

In this research, two types of wood, one from each class, were investigated. Jelutong (*Dyera costulata*) is an imported hardwood from Malaysia that is used mainly for its latex production for chewing gum. With a low density and easy workability, jelutong is ideal for infiltration of oxide sols and molten silicon in a complex-shaped component. Eastern white pine (*Pinus strobus*), a softwood, is typically used as a structural element [15]. In this paper, wood pyrolysis, infiltration behavior, and microstructure of biomorphic ceramics made from jelutong and pine will be presented.

Experimental Procedures

One block of jelutong and three blocks of pine were dried in an oven at 100°C and pyrolyzed in an argon atmosphere. Pyrolysis is the decomposition of a wood heated in an inert atmosphere to release volatiles, leaving behind a carbonaceous preform with cell-like structures. The jelutong blocks measured 15 cm x 4.5 cm x 4.5 cm while the dimensions of the pine blocks were 14 cm x 3.5 cm x 3 cm. The blocks were placed in a Thermcraft tube furnace and pyrolyzed up to 1000°C. Afterwards, the blocks were cut into approximately 0.4 cm thick slices that were to be infiltrated. To investigate the effects of higher pyrolysis temperatures on the pore structure, samples of jelutong and pine were heat-treated at 1400°C and 1800°C for one hour after pyrolysis.

A characterization of the pyrolysis process was performed using thermogravimetry (TG) and differential scanning calorimetry (DSC). These two techniques were executed simultaneously to measure the change in sample mass with temperature as well as changes in enthalpy that occur during pyrolysis. The Netzsch Thermische Analyse STA 409C was used in this process, with alumina powder as the reference sample.

The carbonaceous preforms were infiltrated with Si at 1460°C for one hour in a vacuum Centorr Furnace. Both carbon and SiC samples were infiltrated with ZrO_2 sol in a Buehler Vacuum Impregnation chamber. After infiltration, the samples were dried in a furnace at 85°C for several hours and then placed in a tube furnace for calcination up to 400°C. This process was repeated up to five times. To gain knowledge of the progress of the infiltration, some samples were infiltrated only one or three times.

The original pore structure of the two types of wood were analyzed by viewing a fresh fracture surface of jelutong and pine using the scanning electron microscope (SEM). Images were taken of two orientations of the carbon structures: perpendicular and parallel to the growth direction of the tree. The growth direction is equivalent to the longitudinal axis of the trunk. The SEM was also used for the analysis of the carbon preforms infiltrated with ZrO_2, the porous SiC coated with ZrO_2 (one, three, and five times), and

samples heat-treated at 1800°C. Si and SiC were not readily distinguishable in the SEM images; therefore the samples infiltrated with only Si were viewed with the light optical microscope (LOM). The LOM was also used to characterize the porous SiC samples coated with ZrO_2.

The phases present in the samples that were infiltrated three times with ZrO_2 were determined using X-ray diffraction on samples ground to a powder using a mortar and pestle. The heat-treated samples were also analyzed to determine the nature of carbon in pyrolyzed wood.

Microhardness tests were performed using a Knoop indenter with a 500 g load to measure the hardness in the following regions: reaction formed SiC, Si, and the interface of SiC and Si. A total of six samples were tested: pine (perpendicular to the growth direction), jelutong (perpendicular and parallel to the growth direction), and three porous SiC samples from jelutong, that were infiltrated with ZrO_2 (one, three, and five times). Five indentations were made in each region and the average Knoop hardness value for each region in each sample was calculated.

Results and Discussion

Pyrolysis: After pyrolysis, the blocks retained their shape, but decreased in size. The pyrolysis shrinkage in jelutong was 25% in dimensions and the total volume decreased by 60%. The dimensions of the blocks of pine decreased roughly by 22%, while the total volume was reduced by 50%. Cracks appeared in the pine blocks due to shrinkage stress created from the exterior of the blocks decomposing at a faster rate than the middle, but did not appear in the jelutong block. The heating rates are crucial to the integrity of the pyrolyzed blocks, and each type of wood requires different rates that are dependent on the wood's density [14].

Thermal Analysis: The TG curves for both woods are plotted on the same graph for comparison and are shown in Figure 1. Figure 2 is a plot of both DSC curves. As can be

seen from both TG curves, the majority of the mass loss during pyrolysis occurred between 200°C and 400°C. The peaks in the DSC curves indicate that the reactions and gas evolutions during pyrolysis occur in the same temperature range of 200°C to 400°C. Similarities in the pyrolysis process exist between the woods. The initial weight loss begins around 100°C, where the moisture is removed, and ends at about 170°C. The second step in the weight loss process occurs by the decomposition of hemicellulose (190-280°C) and the release of volatile products. At a slightly higher temperature range of 280-500°C, a majority of the weight loss occurs due to the decomposition of cellulose and lignin, leaving behind a carbon preform. After 500°C, very little weight loss occurs, which can be seen in Figure 2. DSC curves demonstrate the endothermic and exothermic nature of the reactions. While the TGA curves are quite similar for both woods, the DSC curves have slight variations due to the varying chemical composition between jelutong and pine [16]. Details on the reactions can be found in the literature [13].

Porous C and SiC: The microstructure of the pyrolyzed woods and Si infiltrated samples are shown in Figures 3-6. In Figures 3 and 4, the white outlines are carbon and the black areas are the pores. Figure 3a shows that pyrolyzed jelutong has a non-uniform pore structure, with sets of large pores within surrounding smaller pores of varying size. The ray cells in jelutong are evident in Figure 3b, which shows the view that is parallel to the direction of tree growth.

The amount of ray cells in pine (Figure 4b) is less than in jelutong, indicating that the strength of pine would be higher than jelutong in the direction that is perpendicular to the growth. Figure 4a shows that pine has a uniform pore structure, since the pores are similar in size and shape.

When the carbon preforms were infiltrated with silicon, the silicon reacted with the carbon to form silicon carbide (SiC). In Figures 5 and 6, the dark gray outlines represent the SiC, while the light gray areas are excess silicon. The reacted SiC retained the original structure of the wood. Some of the large pores were not completely filled with Si, therefore the final material is not completely dense. Density variation existed across

all of the infiltrated samples, which would affect the results of the hardness tests. Upon further treatment, the excess silicon can be removed, leaving behind a porous SiC structure.

The carbon samples heat-treated at 1800°C are shown in Figure 7. At 1400°C, no changes in structure were apparent, but at the higher temperature, the cell walls underwent a shape transformation. Partial graphitization occurred at 1800°C and with the ordering of the carbon structure, the pore morphology changed slightly and decreased in diameter by an average of roughly 20%. This occurrence would come into effect if the infiltration process of other materials were performed at higher temperatures than 1500°C. The orientation of the graphite may influence the mechanical properties of the final product [17].

Infiltration of sols in C and SiC: Jelutong samples infiltrated with ZrO_2 three and five times are shown in Figures 8a and 8b, respectively. The original structure of jelutong can still be seen, but ZrO_2 now coats it and the pores are filled with crystallized ZrO_2. As the number of infiltrations increased, the amount of oxide deposition increased, eventually completely filling the pores. The same trend was observed in the pine samples infiltrated with ZrO_2 three and five times. The results of these infiltrations can be seen in Figures 9a and 9b. As with three infiltrations in jelutong, the original structure of pine can still be seen, but after five infiltrations, cracks formed in the structure.

Prior to the carbon samples being infiltrated, the preforms had similar physical densities around 0.3 g/cm^3, determined by measuring the dimensions and weight of the sample. After the third infiltration, however, the amount of mass gain of pine leveled off while jelutong continued to accumulate mass. The large sets of pores in the jelutong structure provided additional areas for the ZrO_2 infiltration even after the smaller pores were filled. Figure 10 is a plot of the geometric densities of jelutong and pine after each infiltration. The final densities of the materials vary depending on the type of wood selected for the precursor material. It is controlled by the microstructure of the wood.

SiC samples from jelutong were also infiltrated with ZrO_2 one, three, and five times. After the silicon infiltration, the large pores were not completely filled, so the oxide mostly deposited in the large pores, as well as coated the SiC structure. As the number of these infiltrations increased, the amount of ZrO_2 in the large pores increased, which can be seen in Figure 11.

X-Ray Diffraction: The carbon samples infiltrated with ZrO_2 three times were analyzed by X-ray diffraction to determine the phases present. Both types of wood produced the same results. A plot of the intensity of the beam versus the Bragg angle is shown in Figure 12. The phase predominantly present was monoclinic ZrO_2, but traces of cubic ZrO_2 were also detected.

Without heat-treatment at higher temperatures, the samples consisted of amorphous carbon that was indistinguishable from the sample holder during x-ray diffraction. Scans of the heat-treated samples are displayed in Figure 13, along with the scan of the sample holder for reference. As the heat-treatment temperature increased, the peaks became more defined due to the atomic ordering of the carbon [17].

Microhardness: The average values from the microhardness tests are displayed in Table I and plotted in Figure 14. The average Knoop hardness values for the ZrO_2-coated SiC decreased from 1500 Hk to 1400 Hk as the number of oxide infiltrations increased, as expected due to the softer oxide coating. The lowest hardness value for SiC in the jelutong sample tested parallel to the growth direction is believed to be attributable to the orientation of the fibers. Wood is an anisotropic material whose properties are dependent upon the direction of the loading, leading to a preferred orientation of the porous structure.

The total average Knoop hardness value of all SiC areas was 1510 Hk, which is significantly lower than the documented value of 2480 Hk, possibly due to the difference in densities of the infiltrated sample and monolithic SiC [18]. Indentations in pure SiC were hard to perform due to the size of the SiC areas relative to the size of the indenter;

therefore, accurate hardness values were difficult to obtain. The areas filled with excess Si were larger in size, making indentations in pure Si easier to make. The total average Knoop hardness value for Si was 920 Hk, which is closer in range to the recorded hardness values of 950-1150 Hk [19]. At the interface of SiC and Si, the total average Knoop hardness value fell in between the values of SiC and Si, as expected, at 1230 Hk.

Conclusions

Ecoceramics provide opportunities for expanded designs and applications since they have near-net and complex shape capabilities, variable microstructures, are friendly to the environment, and are economically favorable in comparison with traditional ceramics. Starting with natural wood, the desired final shape of the component can be obtained, and retains that shape all through the process. The microstructure of the original biostructure is maintained throughout the procedure, which allows for knowledge of the resulting properties of the product. Finally, the starting materials used are inexpensive and a renewable resource.

Acknowledgements

The author would like to thank Richard Dacek, John Setlock, Ralph Garlick, and Myles McQuater for their technical assistance. Technical discussions with Professor Julian Martinez-Fernandez and the critical review of the manuscript by Mr. James D. Kiser are also acknowledged.

References

[1] J.E. Mark and P.D. Calvert. "Biomimetic, Hybrid and In-Situ Composites." Mater. Sci. and Engg., C1, 159 (1994).

[2] T. Ota, M. Takahashi, T. Hibi, M. Ozawa, and H. Suzuki. "Biomimetic Process for Producing SiC Wood." J. Am. Ceram. Soc., 78 (1995) 3409.

[3] P. Greil, T. Lifka, and A. Kaindl. "Biomorphic Silicon Carbide Ceramics from Wood: I and II." J. Eur. Ceram. Soc., 18, (1998) 1961.

[4] P. Griel. "Biomorphic Ceramics from Lignocellulosics." J. Eur. Ceram. Soc., 21 (2001) 105-118.

[5] H. Sieber, C. Hoffmann, A. Kaindl, P. Greil. Biomorphic Cellular Ceramics, Advanced Engineering Materials, Vol. 2, No. 3, (2000) pp. 105-109.

[6] D.-W. Shin, S.S. Park, Y.-H. Choa and K. Niihara. "Silicon/Silicon Carbide Composites Fabricated by Infiltration of a Silicon Melt into Charcoal." J. Am. Ceram. Soc., 82, 3251 (1999).

[7] D.C. Nagle and C.E. Byrne. "Carbonized Wood and Materials Formed Therefrom." US Patent 6,124,028 (2000).

[8] M. Singh. "Environment Conscious Ceramics (Ecoceramics)." Ceram. Sci. Engg. Proc., 21 [4] 39-44 (2000).

[9] J. Martinez-Fernandez, F.M. Valeria-Feria and M. Singh. "High Temperature Compressive Mechanical Behavior of Biomorphic Silicon Carbide Ceramics." Scripta Materialia, 43, 813-818 (2000).

[10] G. Qiao, R. Ma, N. Cai, C. Zhang, and Z. Jin. "Mechanical Properties and Microstrucutre of Si/SiC Materials Derived from Native Wood." Materi. Sci. Engg., A 323 (2002) 301-305.

[11] M. Singh. "Environment Conscious Ceramics (Ecoceramics)." NASA/TM-2001-210605, NASA Glenn Research Center, Cleveland, OH.

[12] M. Singh. "Ecoceramics: Ceramics from Wood." Advanced Materials and Processes, March 2002, ASM International, Materials Park, OH.

[13] S. Sinha, A. Jhalani, M.R. Ravi, A. Ray, Modeling of Pyrolysis in Wood: a Review, SESI Journal 10(1), 2000, pp. 41-62.

[14] C.E. Byrne, D.C. Nagle. "Carbonization of Wood for Advanced Materials Applications." Carbon, Vol. 35, No. 2, 1997, pp. 259-266.

[15] Wood Handbook - Wood as an Engineering Material. Forest Products Laboratory. 1999. Gen. Tech. Rep. FPL-GTR-113. Madison, WI: U.S. Department of Agriculture, Forest Service, Forest Products Laboratory. 463 p.

[16] M. Singh and J.A. Salem. "Mechanical Properties and Microstructure of Biomorphic Silicon Carbide Ceramics Fabricated from Wood Precursors." J. Eur. Ceram. Soc., Vol. 22, Nos.14-15, 2002, pp. 2709-1718.

[17] C.E. Byrne, D.C. Nagle. "Carbonized Wood Monoliths – Characterization." Carbon Vol. 35, No. 2, 1997, pp. 267-273.

[18] University of Michigan, Knoop Hardness Number, KHN http://www.lib.umich.edu/dentlib/Dental_tables/Knoophard.html

[19] W.R. Runyan. Silicon Semiconductor Technology. New York, McGraw-Hill Book Company, 1965.

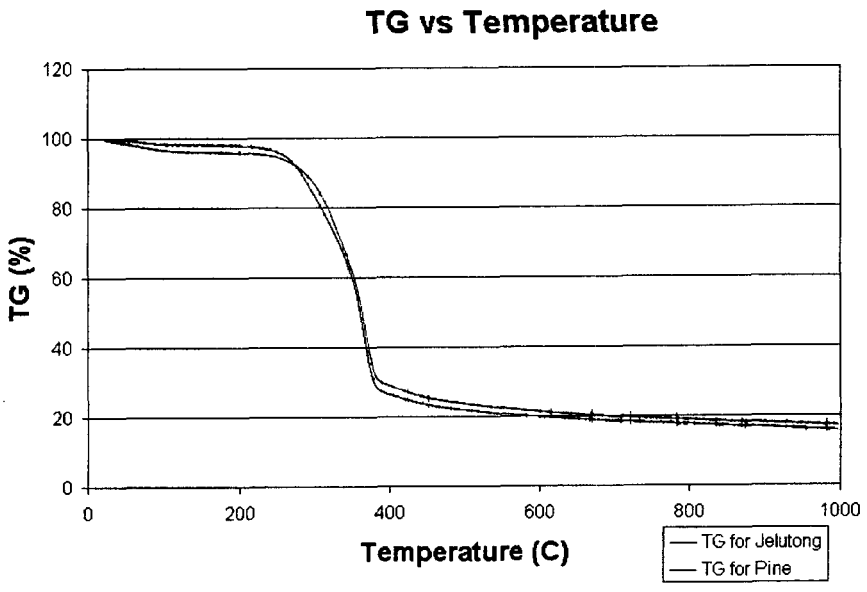

Figure 1. Thermogravimetry curves for jelutong and pine wood.

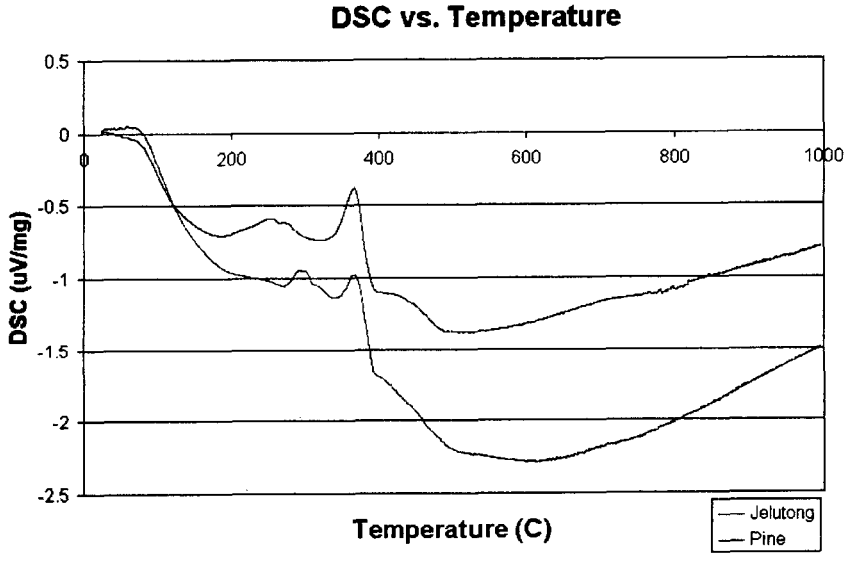

Figure 2. Differential Scanning Calorimetry (DSC) curves for jelutong and pine wood.

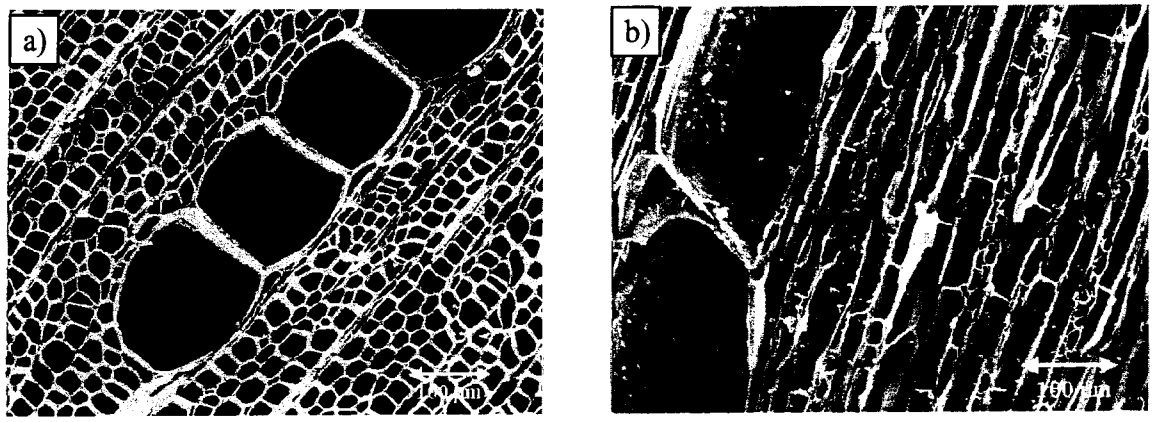

Figure 3. Microstructure of pyrolyzed jelutong in a) axial direction and b) radial direction.

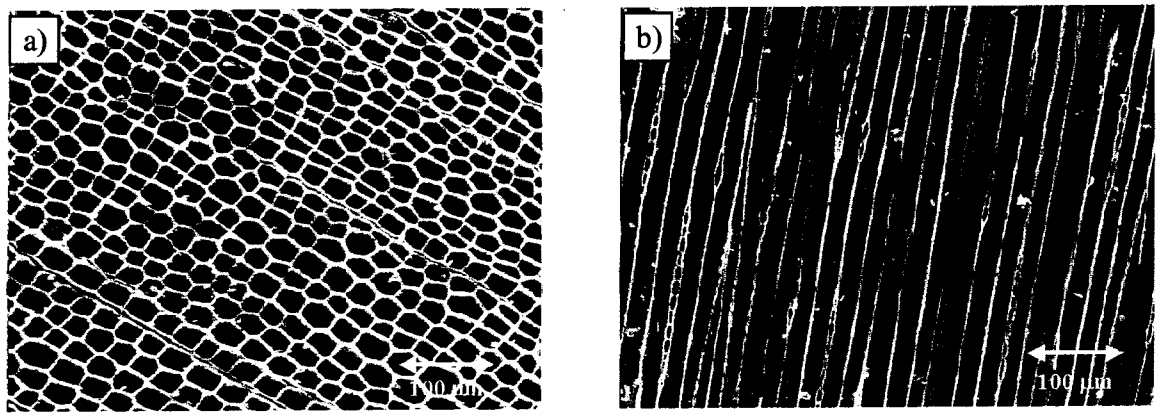

Figure 4. Microstructure of pyrolyzed pine in a) axial direction and b) radial direction.

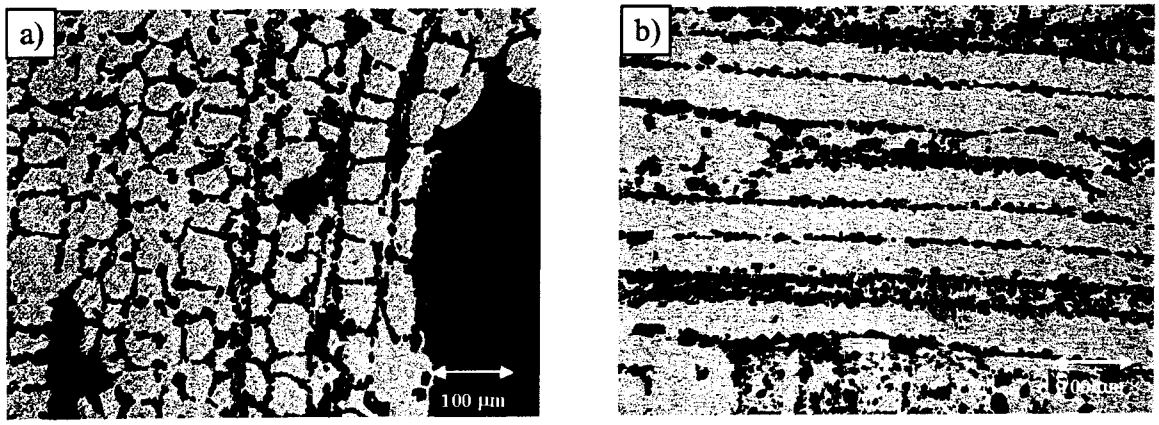

Figure 5. Microstructure of jelutong infiltrated with molten Si in a) axial direction and b) radial direction.

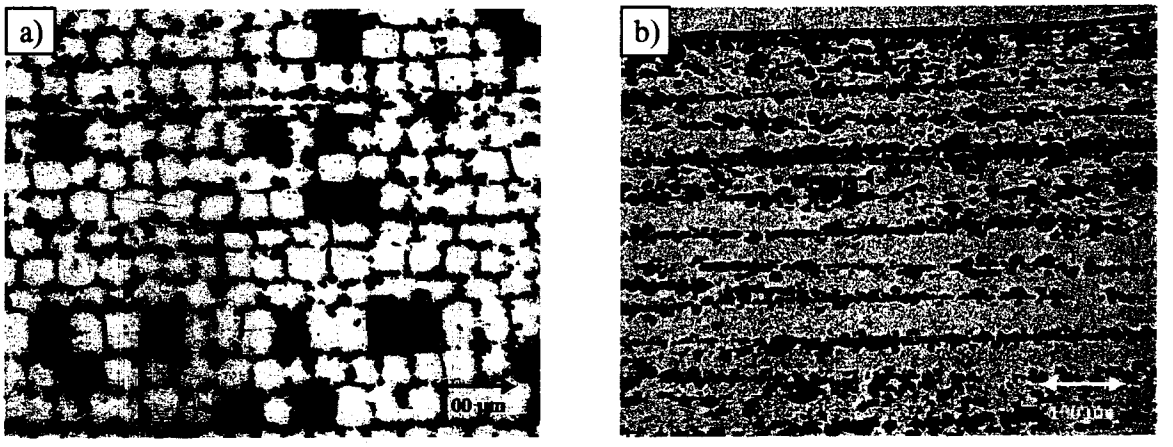

Figure 6. Microstructure of pine infiltrated with molten Si in the a) axial direction and b) radial direction.

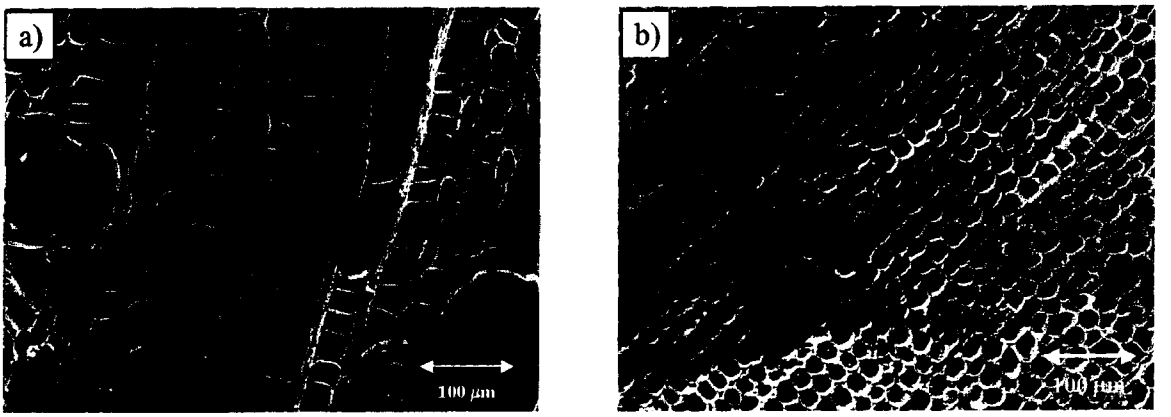

Figure 7. Microstructure of pyrolyzed a) jelutong and b) pine heat treated at 1800° C.

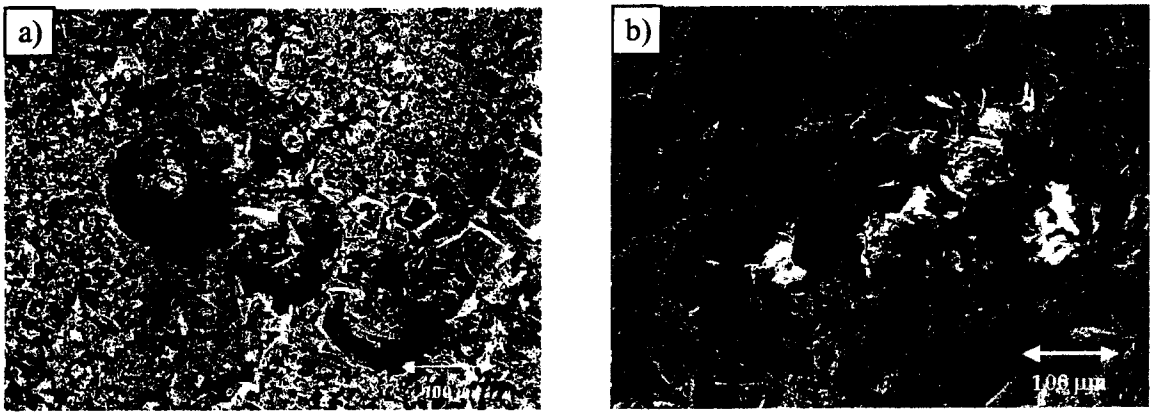

Figure 8. Microstructure of jelutong infiltrated with ZrO_2 a) 3 and b) 5 times in the axial direction.

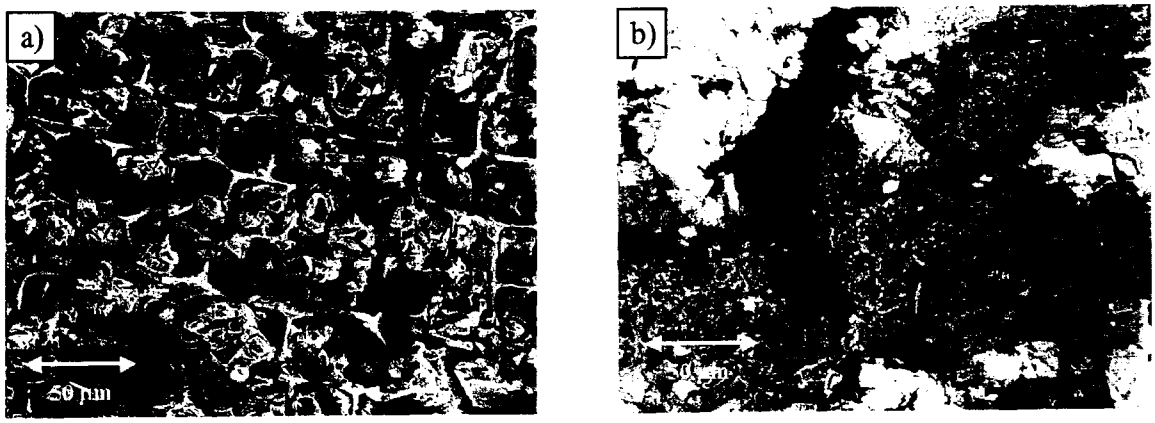

Figure 9. Microstructure of pine infiltrated with ZrO_2 a) 3 and b) 5 times in the axial direction.

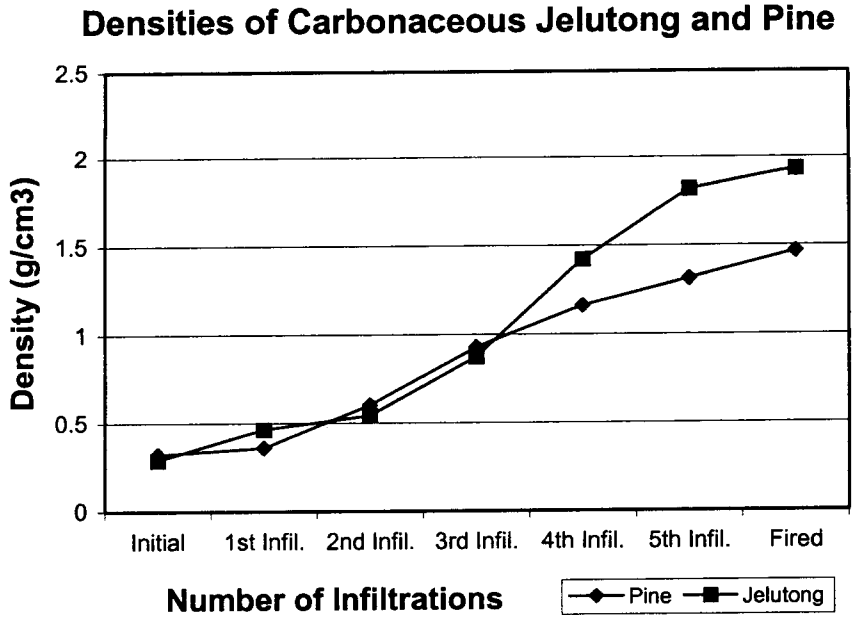

Figure 10. Plot of the densities of carbonaceous jelutong and pine after each infiltration of ZrO_2.

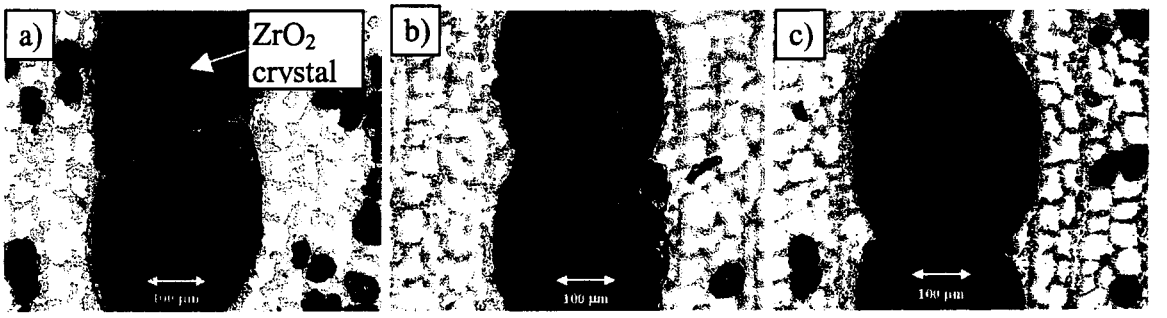

Figure 11. Microstructure of jelutong based SiC infiltrated with ZrO_2 a) one, b) three, and c) five times.

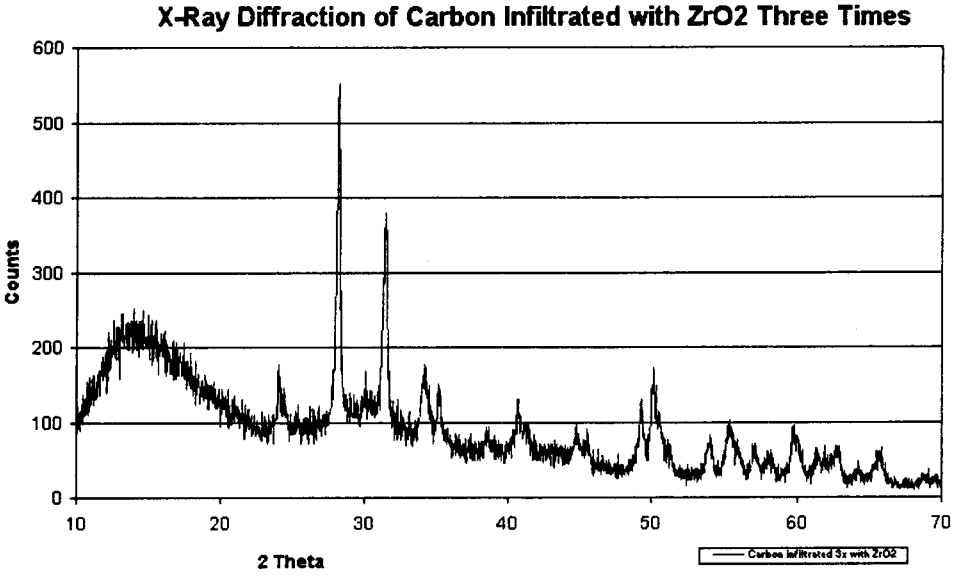

Figure 12. X-ray diffraction scan of carbon preform infiltrated with ZrO_2 three times.

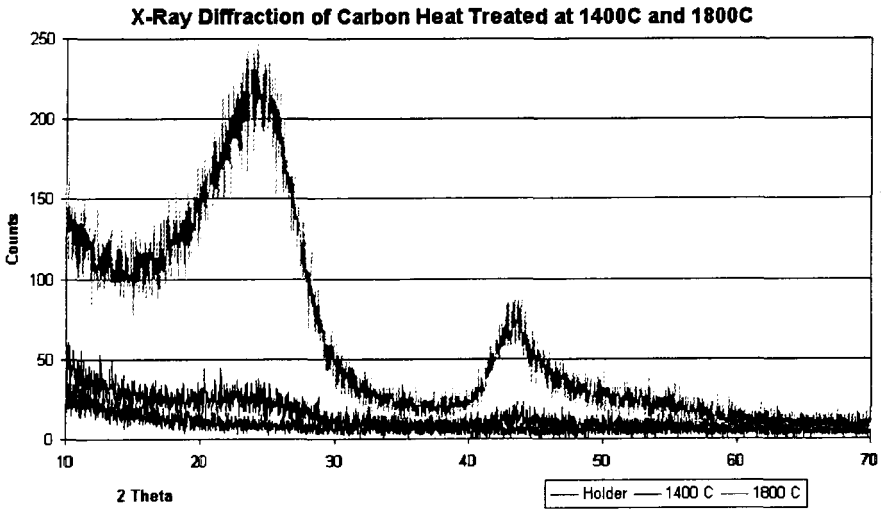

Figure 13. X-ray diffraction scans of samples heat treated at 1400°C and 1800°C with the carbon sample holder as reference.

Table I. Average Knoop hardness values for tested region in each sample.

	Average Knoop Hardness Value		
Sample	SiC region (Hk)	Si Region (Hk)	Interface (Hk)
Pine, $\parallel$ to growth direction	1640	1010	1440
Jelutong, $\perp$ to growth direction	1720	965	1330
Jelutong, $\parallel$ to growth direction	1300	942	1310
Jelutong, (SiC, 1x ZrO_2 infiltrated)	1490	876	1110
Jelutong, (SiC, 3x ZrO_2 infiltrated)	1490	860	1120
Jelutong, (SiC, 5x ZrO_2 infiltrated)	1400	880	1050
Total Average	1510	920	1230
Documented Values	2450	950-1150	

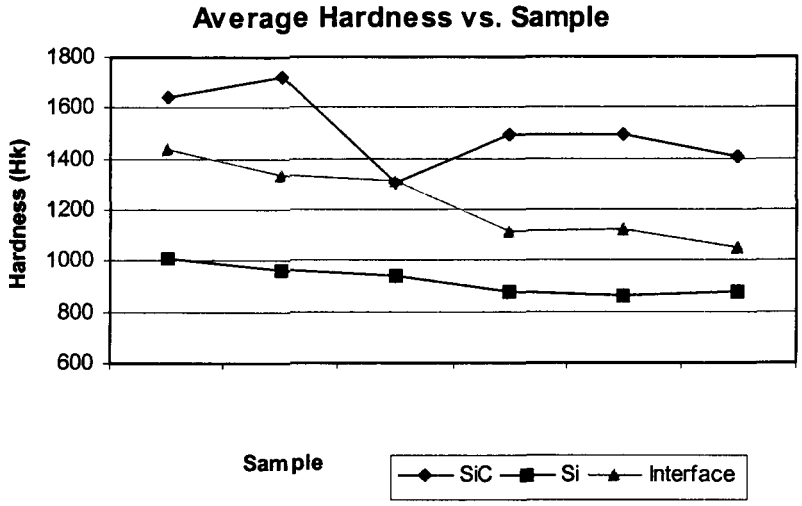

Figure 13. Plot of average Knoop hardness values of SiC, Si, and the interface of each sample.